Estimation of Real Valued Impulse Responses based on Noisy Magnitude and Phase Measurements

Oliver Lang and Mario Huemer
Institute of Signal Processing
Johannes Kepler University
4040 Linz, Austria
oliver.lang@jku.at; mario.huemer@jku.at

Victor Elvira
IMT Lille Douai
Villeneuve d'Ascq 59653, France
victor.elvira@telecom-lille.fr

***Abstract*—We discuss the task of estimating real valued impulse responses based on frequency response measurements. These measurements are available in form of noisy magnitude and phase measurements conducted at discrete frequencies. While this is in general a non-linear estimation problem, it can also be approximated by a linear model, however with noise statistics that depend on the unknown parameters to be estimated. We investigate and compare different types of newly proposed as well as standard classical and Bayesian estimators such as widely linear, maximum likelihood, maximum a posteriori and Monte Carlo based estimators.**

I. Introduction

This work deals with the classic non-linear problem of estimating the real valued impulse response of a linear time-invariant (LTI) system based on noisy magnitude and phase response measurements, which appears in many practical scenarios. We apply newly proposed [1] as well as novel estimators and compare their performances.

We begin with some preliminary definitions and assumptions. The analog real valued impulse response is denoted as $h(t)$. We are interested in estimating the sampled impulse response $h[n] = h(nT_S)$, where T_S is the sampling period. We assume T_S is chosen such that the sampling theorem is practically fulfilled, and we furthermore assume the sampled impulse response to be practically zero after $N_{\mathbf{h}}$ samples. The samples are stacked in a vector $\mathbf{h} \in \mathbb{R}^{N_{\mathbf{h}}\times 1}$. The measurements are given by $N_{\mathbf{y}}$ magnitude and phase response measurements at equidistant frequencies $f_k = k\Delta f$ with $k = 0, \cdots, N_{\mathbf{y}} - 1$. The true magnitude and phase response values of the analog LTI system at frequency f_k are denoted as A_k and φ_k, respectively, with $A_k \in \mathbb{R}_0^+$ and $\varphi_k \in [0, 2\pi)$, such that the frequency response $H(f_k)$ is given by

$$H(f_k) = A_k \mathrm{e}^{j\varphi_k}, \quad k = 0, \cdots, N_{\mathbf{y}} - 1, \tag{1}$$

which corresponds to a transformation from polar coordinates to Cartesian coordinates.

We now define

$$H_{\mathrm{DC}} = \frac{1}{T_S} H(0) \tag{2}$$

$$\mathbf{H}_{\mathrm{AC}} = \frac{1}{T_S} \left[H(f_1), H(f_1), \ldots, H(f_{N_{\mathbf{y}}-1})\right]^T \tag{3}$$

$$\mathbf{H}_{\mathrm{AC,flip}} = \frac{1}{T_S} \left[H(f_{N_{\mathbf{y}}-1}), H(f_{N_{\mathbf{y}}-2}), \ldots, H(f_1)\right]^T \tag{4}$$

and

$$\mathbf{H}_{\mathrm{ds}} = \begin{bmatrix} H_{\mathrm{DC}} & \mathbf{H}_{\mathrm{AC}}^T & \mathbf{H}_{\mathrm{AC,flip}}^H \end{bmatrix}^T \in \mathbb{C}^{N_D \times 1}, \tag{5}$$

with $N_D = 2N_{\mathbf{y}} - 1$. This double-sided discrete frequency response is connected with the sampled impulse response according to

$$\mathbf{H}_{\mathrm{ds}} = \mathbf{F}_{\mathrm{ds}} \mathbf{h}, \tag{6}$$

where $\mathbf{F}_{\mathrm{ds}}$ is the matrix given by the first $N_{\mathbf{h}}$ columns of the discrete Fourier transform (DFT) matrix of size $N_D \times N_D$. We mainly utilize the single-sided frequency response $\mathbf{H}_{\mathrm{ss}}$ defined as

$$\mathbf{H}_{\mathrm{ss}} = \begin{bmatrix} H_{\mathrm{DC}} & \mathbf{H}_{\mathrm{AC}}^T \end{bmatrix}^T = \mathbf{F}_{\mathrm{ss}} \mathbf{h}, \tag{7}$$

where $\mathbf{F}_{\mathrm{ss}}$ is the $N_{\mathbf{y}} \times N_{\mathbf{h}}$ north west submatrix of the DFT matrix of size $N_D \times N_D$. While the connection between the sampled impulse response $\mathbf{h}$ and the discrete frequency response in Cartesian coordinates is linear according to (6) or (7), the relationship between $\mathbf{h}$ and the magnitude- and phase responses A_k and φ_k is non-linear.

II. Measurement Model

At first, we only consider measurements at frequencies $f_k = k\Delta f$ with $k = 1, \cdots, N_{\mathbf{y}} - 1$ and handle the direct current (DC) measurement later on. The magnitude and phase response measurements at frequency f_k are denoted as $y_k^{(A)}$ and $y_k^{(\varphi)}$, respectively. They are related to A_k and φ_k according to

$$y_k^{(A)} = A_k + n_{A,k} \tag{8}$$

$$y_k^{(\varphi)} = \varphi_k + n_{\varphi,k}, \tag{9}$$

where $n_{A,k}$ and $n_{\varphi,k}$ denote the corresponding measurement noise variables, which we assume to be statistically independent. The probability density functions (PDFs) of $n_{A,k}$ and $n_{\varphi,k}$ clearly depend on the measurement method. We assume $n_{\varphi,k}$ to be zero mean Gaussian with variance $\sigma_{\varphi,k}^2$. Since A_k and $y_k^{(A)}$ have to be positive valued, $n_{A,k}$ cannot be zero mean Gaussian. The concrete PDF of $n_{A,k}$, denoted as $p(n_{A,k})$, depends on the utilized measurement method. In this work, we consider the following way of generating the magnitude measurements: First, the magnitude measurements

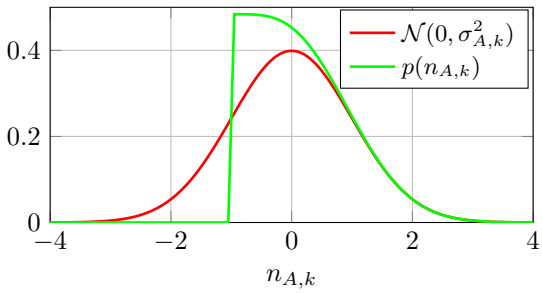

Fig. 1. Exemplarily PDF of the magnitude measurement noise $p(n_{A,k})$ for $A_k = 1$ and $\sigma^2_{A,k} = 1$.

are in a first shot generated by adding white Gaussian noise with zero mean and variance $\sigma^2_{A,k}$ to the true magnitude values. If a magnitude measurement turns out to be negative valued, its sign is changed. In terms of the PDF of the magnitude measurement noise, this manipulation is interpreted the following way: At first, $p(n_{A,k})$ is assumed to be zero mean Gaussian with variance $\sigma^2_{A,k}$. The values corresponding to $n_{A,k} < -A_k$ would result in negative valued magnitude measurements, which are prohibited. Hence, the parts of the PDF corresponding to $n_{A,k} < -A_k$ are mirrored w.r.t. the value $n_{A,k} = -A_k$. Fig. 1 visualizes this manipulation for $A_k = 1$ and $\sigma^2_{A,k} = 1$. Obviously, this PDF does not have zero mean anymore. The resulting mean value of $p(n_{A,k})$ is denoted as $\mu_k = E[n_{A,k}]$ in the following. For large A_k, $p(n_{A,k})$ is approximately zero mean Gaussian with variance $\sigma^2_{A,k}$, however, for small A_k, $p(n_{A,k})$ is not Gaussian and μ_k is not zero. The resulting mean μ_k depends on the true but unknown magnitude response A_k. Note that we assumed the LTI system is approximately band-limited, hence, small values of A_k definitely occur.

Transforming the magnitude and phase response measurements to Cartesian coordinates gives

$$y_k = y_k^{(A)} \mathrm{e}^{j y_k^{(\varphi)}} \tag{10}$$
$$= (A_k + n_{A,k}) \mathrm{e}^{j(\varphi_k + n_{\varphi,k})} \tag{11}$$
$$= A_k \mathrm{e}^{j\varphi_k} \mathrm{e}^{j n_{\varphi,k}} + n_{A,k} \mathrm{e}^{j\varphi_k} \mathrm{e}^{j n_{\varphi,k}}. \tag{12}$$

The random variable y_k can be written as the sum of its mean and a zero mean noise term according to

$$y_k = E[y_k] + n_k. \tag{13}$$

From (12), the mean $E[y_k]$ follows to

$$E[y_k] = A_k \mathrm{e}^{j\varphi_k} E\left[\mathrm{e}^{j n_{\varphi,k}}\right] + \mu_k \mathrm{e}^{j\varphi_k} E\left[\mathrm{e}^{j n_{\varphi,k}}\right] \tag{14}$$
$$= \alpha_k H(f_k) + \alpha_k \mu_k \mathrm{e}^{j\varphi_k}, \tag{15}$$

where $\alpha_k = E\left[\mathrm{e}^{j n_{\varphi,k}}\right] = E[\cos(n_{\varphi,k})] = \mathrm{e}^{-\sigma^2_{\varphi,k}/2} \in [0, 1]$ for $n_{\varphi,k} \sim \mathcal{N}(0, \sigma^2_{\varphi,k})$ [2].

We now turn to the noise term n_k in (13). There exists some literature on how noise statistics can be transformed from a polar into a Cartesian coordinate system such as [3] for the application of tracking in 2D and 3D spaces. Other techniques that incorporate noise statistics are often based on the unscented transform [4] as in [5], [6]. However, there exist some major differences between existing methods and the way the problem is tackled in this work. The biggest difference is that the range measurements in tracking applications (which correspond to the magnitude measurements in this work) are often assumed to be large. Hence, the corresponding range measurement noise is often considered to be a zero mean Gaussian random variable. In this work, A_k may be very small and μ_k may not be zero. This circumstance affects not only the mean $E[y_k]$ according to (15) but also the noise term n_k in (13). To show this, the variance σ_k^2 and pseudo-variance $\tilde{\sigma}_k^2$ of n_k for $1 \leq k \leq N_{\mathbf{y}} - 1$ of n_k are derived in Appendix A and are given by

$$\sigma_k^2 = E[(y_k - E[y_k])(y_k - E[y_k])^*] \tag{16}$$
$$= A_k^2(1 - \alpha_k^2) + 2A_k\mu_k(1 - \alpha_k^2) - \alpha_k^2\mu_k^2 + \eta_k \tag{17}$$

and

$$\tilde{\sigma}_k^2 = E[(y_k - E[y_k])(y_k - E[y_k])] \tag{18}$$
$$= \mathrm{e}^{j2\varphi_k}(A_k^2\beta_k + \eta_k\beta_k + 2A_k\mu_k\beta_k - 2\alpha_k^2 A_k^2 - 2\alpha_k^2 A_k\mu_k), \tag{19}$$

respectively, where $\beta_k = E\left[\mathrm{e}^{j2n_{\varphi,k}}\right] = E[\cos(2n_{\varphi,k})] = \mathrm{e}^{-4\sigma^2_{\varphi,k}/2} \in [0, 1]$ and where $\eta_k = E[n^2_{A,k}]$. Since α_k and β_k depend on $\sigma^2_{\varphi,k}$ only, they are considered to be given. It is important to note that the noise statistics in (17) and (19) depend on the true magnitude and phase response values A_k and φ_k [2], [3]. Hence, the true statistics cannot be evaluated without knowing the true magnitude and phase response values. An obvious option is to replace A_k and φ_k by $y_k^{(A)}$ and $y_k^{(\varphi)}$ in (17) and (19). Also note that η_k corresponds to the variance of the magnitude measurement noise $\sigma^2_{A,k}$ only for the case when μ_k is zero, which is not always the case.

We now turn to the measurement at DC, which can be performed by measuring the steady state system response for a unit step at the input. Instead of a magnitude and a phase, the measurement at DC is simply given by a real (positive or negative) scalar value denoted by y_0. We assume the measurement noise at DC to be zero mean Gaussian with variance $\sigma_0^2 = \sigma^2_{A,0}$ and pseudo-variance $\tilde{\sigma}_0^2 = \sigma_0^2$. These settings correspond to real valued noise samples.

By defining y_{DC}, $\mathbf{y}_{\mathrm{AC}}$ and $\mathbf{y}_{\mathrm{ss}}$ according to the rules in (2)–(5) and (7) we finally end up at the compact measurement model

$$\mathbf{y}_{\mathrm{ss}} = \underbrace{\mathbf{D}\mathbf{F}_{\mathrm{ss}}}_{\mathbf{H}} \mathbf{h} + \mathbf{n} \tag{20}$$
$$= \mathbf{H}\mathbf{h} + \mathbf{n}, \tag{21}$$

where $\mathbf{D} \in \mathbb{R}^{N_{\mathbf{y}} \times N_{\mathbf{y}}}$ is a diagonal matrix with $[\mathbf{D}]_{1,1} = 1$ and $[\mathbf{D}]_{k+1,k+1} = \alpha_k$ for $k = 1, \cdots, N_{\mathbf{y}} - 1$. Assuming the measurements for different k to be statistically independent, the noise covariance matrix $\mathbf{C_{nn}}$ and the pseudo-noise covariance matrix $\tilde{\mathbf{C}}_{\mathbf{nn}}$ follow to be diagonal matrices that can (according to (17) and (19)) be approximated by $[\mathbf{C_{nn}}]_{k+1,k+1} = \sigma_k^2$

and $[\tilde{\mathbf{C}}_{\mathbf{nn}}]_{k+1,k+1} = \tilde{\sigma}_k^2$ for $k = 0, \cdots, N_{\mathbf{y}} - 1$. The non-linear connection between the polar measurements and the sampled impulse response has finally been transformed to the model in (21) that formally looks like a linear model, but which exhibits noise statistics depending on the true magnitude and phase response values A_k and φ_k. The noise statistics consequently depend on the unknown vector $\mathbf{h}$ to be estimated. This dependency is considered by the following estimation methods.

III. Estimation Methods

Note that well-known estimators such as the LS estimator, the best linear unbiased estimator (BLUE) [7] or the best widely linear unbiased estimator (BWLUE) [8], [9] applied on the complex valued vector $\mathbf{y}_{\text{ss}}$ in (21) result in complex valued estimates of the impulse response $\mathbf{h}$. This corresponds to a systematic error since the impulse response is considered to be real valued. In [1], it was shown that considering only the real part of the complex valued estimates for further processing is in general not optimal. Also in [1], optimal methods were derived that produce only real valued estimates. One of these estimators is the widely linear lest squares (WLLS) estimator for real valued parameters.

a) *WLLS estimator for real valued parameters*: This estimator is given by

$$\hat{\mathbf{h}} = \left(\widetilde{\mathbf{H}}^H \widetilde{\mathbf{H}}\right)^{-1} \widetilde{\mathbf{H}}^H \underline{\mathbf{y}}. \tag{22}$$

where $\underline{\mathbf{y}} = \begin{bmatrix}\mathbf{y}_{\text{ss}}^T & \mathbf{y}_{\text{ss}}^H\end{bmatrix}^T$ and where $\widetilde{\mathbf{H}} = \begin{bmatrix}\mathbf{H}^T & \mathbf{H}^H\end{bmatrix}^T$. This estimator is of widely linear form and produces real valued estimates only. Furthermore, it does not incorporate any noise statistics. Thus, it is prone to any errors when approximating the noise statistics.

b) *BWLUE for real valued parameters*: This estimator proposed in [1] is able to incorporate the noise statistics in the form of $\mathbf{C}_{\mathbf{nn}}$ and $\tilde{\mathbf{C}}_{\mathbf{nn}}$ according to

$$\hat{\mathbf{h}} = \left(\widetilde{\mathbf{H}}^H \underline{\mathbf{C}}_{\mathbf{nn}}^{-1} \widetilde{\mathbf{H}}\right)^{-1} \widetilde{\mathbf{H}}^H \underline{\mathbf{C}}_{\mathbf{nn}}^{-1} \underline{\mathbf{y}}, \tag{23}$$

where

$$\underline{\mathbf{C}}_{\mathbf{nn}} = \begin{bmatrix}\mathbf{C}_{\mathbf{nn}} & \tilde{\mathbf{C}}_{\mathbf{nn}} \\ \tilde{\mathbf{C}}_{\mathbf{nn}}^* & \mathbf{C}_{\mathbf{nn}}^*\end{bmatrix}. \tag{24}$$

Since in our application the noise statistics depend on the unknown A_k and φ_k we insert the measurements $y_k^{(A)}$ and $y_k^{(\varphi)}$ in (17) and (19) to obtain approximations of the noise statistics. By doing so, we also set $\mu_k = 0$ and $\eta_k = \sigma_{A,k}^2$. Recall that for the DC measurement we set $\tilde{\sigma}_0^2 = \sigma_0^2$. In fact, this choice makes $\underline{\mathbf{C}}_{\mathbf{nn}}$ utilized in (23) singular. To overcome this problem, we perform $\sigma_0^2 \leftarrow \sigma_0^2 + \gamma$ and $\tilde{\sigma}_0^2 \leftarrow \tilde{\sigma}_0^2 - \gamma$ with an arbitrary positive valued γ. This choice is motivated in [1] and it does not change the estimation results.

c) *Two-step-approach*: Especially when the measurement variances are large, $y_k^{(A)}$ and $y_k^{(\varphi)}$ can deviate heavily from A_k and φ_k, which might lead to bad approximations of the noise statistics in (17) and (19). We therefore apply the following two-step estimation approach [1]: 1) Perform a WLLS estimation, transform the estimated impulse response into frequency domain using a DFT, and use the resulting frequency response values for approximating the noise statistics in (17) and (19). Furthermore, μ_k and η_k are approximated via numerical integration of $p(n_{A,k})$ when replacing A_k by the estimated magnitude response from the WLLS estimation step

$$\mu_k \approx \int_{-\infty}^{\infty} n_{A,k}\, p(n_{A,k})\, \mathrm{d}n_{A,k} \tag{25}$$

$$\eta_k \approx \int_{-\infty}^{\infty} n_{A,k}^2\, p(n_{A,k})\, \mathrm{d}n_{A,k}. \tag{26}$$

2) Apply the BWLUE for real valued parameters with the (usually) more precise noise statistics to obtain an improved impulse response estimate.

d) *Ideal BWLUE*: For the two-step-approach, the noise statistics were approximated by using estimates of A_k and φ_k. A theoretical estimator can be found by evaluating the noise statistics when using the true magnitude and phase response values instead of the estimates. This results in true noise statistics σ_k^2 and $\tilde{\sigma}_k^2$. These statistics can then be utilized by the BWLUE for real valued parameters to obtain an estimate of $\mathbf{h}$. Note that this procedure is only possible in the simulations where the true magnitude and phase response values are known, however, it gives an idea about the performance loss resulting from approximating for σ_k^2 and $\tilde{\sigma}_k^2$.

The following estimator does not utilize the transformed measurements in Cartesian coordinates but rather the plain measurements in polar coordinates. This has the advantage that fewer approximations for evaluating the noise statistics are required, with the drawback that the connection between the measurements and the impulse response becomes non-linear.

e) *Approximate ML estimator*: Recall that the measurements for different k are assumed to be statistically independent. Therefore, the likelihood PDF of all measurements is the product of the likelihood PDFs of every single measurement. Furthermore, the likelihood PDFs of the single measurements are known except for the fact that $p(n_{A,k})$ depends on the unknown magnitude response A_k. However, for a given estimate $\hat{\mathbf{h}}$, $p(n_{A,k})$ can be approximated by replacing A_k with the magnitude response value resulting from applying the DFT on $\hat{\mathbf{h}}$. With this, an approximation of the likelihood PDF is given as a function of $\hat{\mathbf{h}}$. This allows to find an approximate maximum likelihood estimator by simply applying a Newton-based maximization algorithm on the approximated likelihood PDF.

In the following, Bayesian estimators employed in this work are detailed. Since Bayesian estimators require prior knowledge about the unknown impulse response, we assume the prior mean vector $E[\mathbf{h}]$ as well as the prior covariance matrix

$\mathbf{C_{hh}}$ to be given. Since $\mathbf{h}$ is real valued, it holds that $\tilde{\mathbf{C}}_{\mathbf{hh}} = \mathbf{C_{hh}}$.

f) *WLMMSE estimator*: The Bayesian WLMMSE estimator [8], [9] utilizes prior statistics as well as noise statistics and is given in augmented notation by

$$\underline{\hat{\mathbf{h}}} = E[\underline{\mathbf{h}}] + \underline{\mathbf{C}}_{\mathbf{hh}}\underline{\mathbf{H}}^H \left(\underline{\mathbf{H}}\,\underline{\mathbf{C}}_{\mathbf{hh}}\underline{\mathbf{H}}^H + \underline{\mathbf{C}}_{\mathbf{nn}}\right)^{-1} \underline{\mathbf{y}}, \quad (27)$$

where

$$\underline{\mathbf{C}}_{\mathbf{hh}} = \begin{bmatrix} \mathbf{C_{hh}} & \tilde{\mathbf{C}}_{\mathbf{hh}} \\ \tilde{\mathbf{C}}^*_{\mathbf{hh}} & \mathbf{C}^*_{\mathbf{hh}} \end{bmatrix}, \qquad E[\underline{\mathbf{h}}] = \begin{bmatrix} E[\mathbf{h}] \\ E[\mathbf{h}]^* \end{bmatrix}, \quad (28)$$

and

$$\underline{\mathbf{H}} = \begin{bmatrix} \mathbf{H} & \mathbf{0} \\ \mathbf{0} & \mathbf{H}^* \end{bmatrix}. \quad (29)$$

The noise statistics are approximated the same way as for the BWLUE for real valued parameters in b).

g) *Bayesian two-step-approach*: Similar to the estimation method described in c), the WLMMSE estimates can be utilized to increase the accuracy of the noise statistics. Here, the magnitude and phase response values evaluated from the WLMMSE estimates are used to approximate for σ_k^2 and $\tilde{\sigma}_k^2$ in (17) and (19), respectively. Furthermore, the resulting approximation of $p(n_{A,k})$ is used to approximate for μ_k and η_k via numerical integration of (25) and (26), respectively.

h) *Ideal WLMMSE estimator*: In analogy to the ideal BWLUE discussed in d), a theoretical Bayesian estimator can be found when using the true noise statistics σ_k^2 and $\tilde{\sigma}_k^2$ (evaluated with the true magnitude and phase response values). These true statistics are then utilized by the WLMMSE estimator to obtain an estimate of $\mathbf{h}$. This procedure gives an idea about the performance loss resulting from approximating for σ_k^2 and $\tilde{\sigma}_k^2$ in f) and g).

The Bayesian estimators discussed so far do not require the full prior PDF $p(\mathbf{h})$ but rather only the mean vector and the augmented covariance matrix of $\mathbf{h}$. In contrast to that, the approximate MAP estimator discussed in the following requires the knowledge of $p(\mathbf{h})$. Hence, we assume that $\mathbf{h} \sim \mathcal{N}(E[\mathbf{h}], \mathbf{C_{hh}})$.

i) *Approximate MAP estimator*: With the prior PDF being given, a straightforward extension of the approximate ML estimator discussed in e) leads to an approximate MAP estimator. This extension as achieved by multiplying the approximated likelihood PDF from e) with the prior PDF. The resulting (unnormalized) approximated posterior PDF that only depends on $\mathbf{h}$. Hence, a Newton-based maximization algorithm can be employed to find the vector $\mathbf{h}$ that maximizes the approximated posterior PDF.

j) *MC-based Methods*: Monte Carlo allows for the approximation of the posterior distribution (using the same likelihood and prior distribution described above). In particular, adaptive importance sampling (AIS) algorithms implement importance sampling procedure for improving the efficiency iteratively [10]. In this paper, we implement the LR-PMC [11] with $N = 20$ Gaussian proposals, $T = 10$ iterations, and $K = 500$ samples per proposal and iteration. The Gaussian proposals are initialized in the hypercube $[-1, 1]^{N_\mathbf{h}}$, with isotropic covariance with $\mathbf{C}_n = \sigma^2 \mathbf{I}_{N_\mathbf{h}}$ for $n = 1, ..., N$ where $\sigma = 0.2$. Figure X shows the Bayesian estimators when changing the dimension of the problem $N_\mathbf{h}$, in all cases with a Gaussian observation noise with $\sigma = 0.01$. Note than in low dimension, the AIS method performs well. However, when the performance deteriorates with the dimension increase due to the well-known curse of dimensionality. In the future, we plan to apply other AIS methods such as APIS [12] or LAIS [13], or to develop novel AIS methods for this challenging problem.

IV. Simulation Results

The task in the following simulation example it to estimate a real valued impulse responses $\mathbf{h}$ with length $N_\mathbf{h} = 12$ based on $N_\mathbf{y} = 10$ randomly generated noisy magnitude and phase response measurements. The true impulse responses $\mathbf{h}$ were randomly generated by sampling 9 samples from a normal distribution with zero mean and unit variance, which are then filtered with a finite impulse response (FIR) filter whose coefficients are given by

$$\mathbf{f} = \begin{bmatrix} 0.0881 & 0.4408 & 0.4408 & 0.0881 \end{bmatrix}^T. \quad (30)$$

This FIR filter corresponds to a low-pass and it takes care that $\mathbf{h}$ shows low-pass characteristics. Next, the DC- and additional 9 noisy magnitude and phase response measurements are generated as described in Sec. II, such that $N_\mathbf{y} = 10$. In the first experiment the noise variance of the phase response measurements is kept constant at $\sigma^2_{\varphi,k} = 10^{-1}$ for $1 \leq k \leq N_\mathbf{y} - 1$ while the variances $\sigma^2_{A,k}$ are varied between 10^{-5} and 1 for $0 \leq k \leq N_\mathbf{y} - 1$. We compare the estimators listed in Sec. III. Since the true impulse responses are generated randomly, the BMSE is used as a performance measure. The resulting average BMSE curves (averaged over the elements of $\hat{\mathbf{h}}$) of the estimation methods a)–i) plotted over $\sigma^2_{A,k}$ are shown in Fig. 2. There, one can see that the WLLS estimator for real valued parameters, although it is prone to any approximation errors of the noise statistics, performs the worst. A significant increase in performance is achieved by the BWLUE for real valued parameters. Combining these two estimators in form of the two-step-approach results in another increase in performance. This two-step-approach almost achieves the performance bound for widely linear classical estimators, which is given in form of the ideal BWLUE. The best performance, however, is observed for the approximate ML estimator except for very high values of $\sigma^2_{A,k}$.

The Bayesian estimation methods are compared in Fig. 3. This figure shows that the two-step approach significantly outperforms the WLMMSE estimator for almost all values of $\sigma^2_{A,k}$. Furthermore, it nearly reaches the performance bound for widely linear Bayesian estimators given by the ideal WLMMSE estimator. For small values of $\sigma^2_{A,k}$, a further

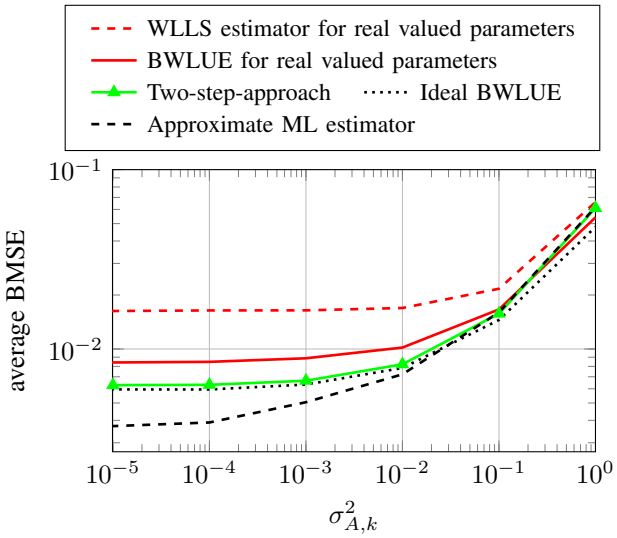

Fig. 2. Average BMSEs of the estimated impulse response coefficients for various classical estimators.

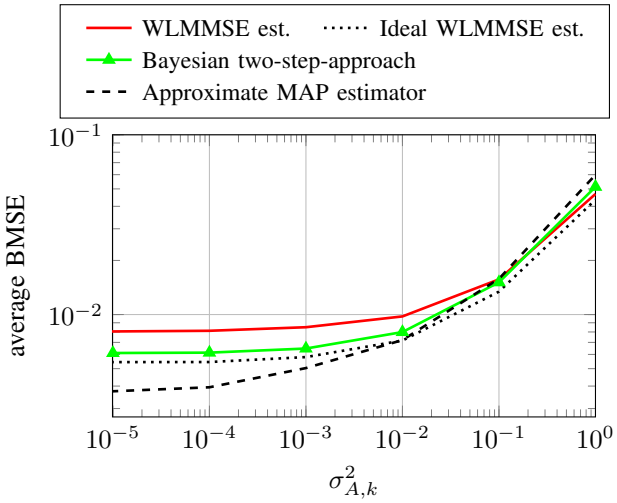

Fig. 3. Average BMSEs of the estimated impulse response coefficients for various Bayesian estimators.

increase in performance can be achieved by utilizing the approximate MAP estimator.

V. Conclusion

We discussed the task of estimating real valued impulse responses based on frequency response measurements. These measurements are available in form of noisy magnitude and phase measurements conducted at discrete frequencies. These polar measurements are connected with the impulse response in a non-linear way. This connection can be approximated by a linear model, however with noise statistics that depend on the unknown parameters to be estimated. We derived the corresponding noise statistics for the linearized model. By doing so, we included the case where the magnitude measurement noise becomes non-Gaussian for small magnitude values. Based on these statistics, we investigated and compared different types of newly proposed as well as standard classical and Bayesian estimation methods. The simulation example presented in this work shows that the approximations of the ML and MAP estimators are superior to the other estimation methods except for large magnitude measurement variances.

APPENDIX A
VARIANCE AND PSEUDO-VARIANCE OF y_k

The variance σ_k^2 of the k^{th} measurement y_k in Cartesian coordinates can be derived as

$$\sigma_k^2 = E\left[(y_k - E[y_k])(y_k - E[y_k])^*\right] \tag{31}$$

$$= E\Big[\left(A_k e^{j\varphi_k} e^{jn_{\varphi,k}} + n_{A,k} e^{j\varphi_k} e^{jn_{\varphi,k}} - \alpha_k A_k e^{j\varphi_k} - \alpha_k \mu_k e^{j\varphi_k}\right) \cdot \left(A_k e^{-j\varphi_k} e^{-jn_{\varphi,k}} + n_{A,k} e^{-j\varphi_k} e^{-jn_{\varphi,k}} - \alpha_k A_k e^{-j\varphi_k} - \alpha_k \mu_k e^{-j\varphi_k}\right)\Big] \tag{32}$$

$$= E\Big[A_k^2 + A_k n_{A,k} - \alpha_k A_k^2 e^{jn_{\varphi,k}} - \alpha_k \mu_k A_k e^{jn_{\varphi,k}} + A_k n_{A,k} + n_{A,k}^2 - \alpha_k A_k n_{A,k} e^{jn_{\varphi,k}} - \alpha_k \mu_k n_{A,k} e^{jn_{\varphi,k}} - \alpha_k A_k^2 e^{-jn_{\varphi,k}} - \alpha_k A_k n_{A,k} e^{-jn_{\varphi,k}} + \alpha_k^2 A_k^2 + \alpha_k^2 \mu_k A_k - \alpha_k A_k \mu_k e^{-jn_{\varphi,k}} - \alpha_k n_{A,k} \mu_k e^{-jn_{\varphi,k}} + \alpha_k^2 \mu_k A_k + \alpha_k^2 \mu_k^2\Big] \tag{33}$$

$$= A_k^2 + A_k \mu_k - \alpha_k^2 A_k^2 - \alpha_k^2 A_k \mu_k + A_k \mu_k + E[n_{A,k}^2] - \alpha_k^2 A_k \mu_k - \alpha_k^2 \mu_k^2 - \alpha_k^2 A_k^2 - \alpha_k^2 A_k \mu_k + \alpha_k^2 A_k^2 + \alpha_k^2 A_k \mu_k - \alpha_k^2 A_k \mu_k - \alpha_k^2 \mu_k^2 + \alpha_k^2 A_k \mu_k + \alpha_k^2 \mu_k^2 \tag{34}$$

$$= A_k^2(1 - \alpha_k^2) + 2A_k \mu_k (1 - \alpha_k^2) - \alpha_k^2 \mu_k^2 + E[n_{A,k}^2]. \tag{35}$$

With the notation $\eta_k = E[n_{A,k}^2]$, this result reads as

$$\sigma_k^2 = A_k^2(1 - \alpha_k^2) + 2A_k \mu_k (1 - \alpha_k^2) - \alpha_k^2 \mu_k^2 + \eta_k. \tag{36}$$

Similarly, the pseudo-variance $\tilde{\sigma}_k^2$ of the k^{th} measurement y_k in Cartesian coordinates follows as

$$\tilde{\sigma}_k^2 = E\left[(y_k - E[y_k])(y_k - E[y_k])\right] \tag{37}$$

$$= E\Big[\left(A_k e^{j\varphi_k} e^{jn_{\varphi,k}} + n_{A,k} e^{j\varphi_k} e^{jn_{\varphi,k}} - \alpha_k A_k e^{j\varphi_k} - \alpha_k \mu_k e^{j\varphi_k}\right) \cdot \left(A_k e^{j\varphi_k} e^{jn_{\varphi,k}} + n_{A,k} e^{j\varphi_k} e^{jn_{\varphi,k}} - \alpha_k A_k e^{j\varphi_k} - \alpha_k \mu_k e^{j\varphi_k}\right)\Big] \tag{38}$$

$$= e^{j2\varphi_k} E\Big[\left(A_k e^{jn_{\varphi,k}} + n_{A,k} e^{jn_{\varphi,k}} - \alpha_k A_k - \alpha_k \mu_k\right)\left(A_k e^{jn_{\varphi,k}} + n_{A,k} e^{jn_{\varphi,k}} - \alpha_k A_k - \alpha_k \mu_k\right)\Big] \tag{39}$$

$$= e^{j2\varphi_k} E\Big[A_k^2 e^{j2n_{\varphi,k}} + A_k n_{A,k} e^{j2n_{\varphi,k}} - \alpha_k A_k^2 e^{jn_{\varphi,k}} - \alpha_k \mu_k A_k e^{jn_{\varphi,k}} + A_k n_{A,k} e^{j2n_{\varphi,k}} + n_{A,k}^2 e^{j2n_{\varphi,k}} - \alpha_k A_k n_{A,k} e^{jn_{\varphi,k}} - \alpha_k \mu_k n_{A,k} e^{jn_{\varphi,k}} - \alpha_k A_k^2 e^{jn_{\varphi,k}} - \alpha_k A_k n_{A,k} e^{jn_{\varphi,k}} + \alpha_k^2 A_k^2 + \alpha_k^2 \mu_k A_k - \alpha_k A_k \mu_k e^{jn_{\varphi,k}} - \alpha_k n_{A,k} \mu_k e^{jn_{\varphi,k}} + \alpha_k^2 \mu_k A_k + \alpha_k^2 \mu_k^2\Big] \tag{40}$$

$$= e^{j2\varphi_k}\Big(A_k^2 E[e^{j2n_{\varphi,k}}] + A_k \mu_k E[e^{j2n_{\varphi,k}}] - \alpha_k^2 A_k^2 - \alpha_k^2 A_k \mu_k + A_k \mu_k E[e^{j2n_{\varphi,k}}] + E[n_{A,k}^2] E[e^{j2n_{\varphi,k}}] - \alpha_k^2 A_k \mu_k - \alpha_k^2 \mu_k^2 - \alpha_k^2 A_k^2 - \alpha_k^2 A_k \mu_k + \alpha_k^2 A_k^2 + \alpha_k^2 A_k \mu_k - \alpha_k^2 A_k \mu_k - \alpha_k^2 \mu_k^2 + \alpha_k^2 A_k \mu_k + \alpha_k^2 \mu_k^2\Big). \tag{41}$$

By donating $\beta_k = E[e^{j2n_{\varphi,k}}]$ and utilizing the definition of η_k, this result transforms to

$$\tilde{\sigma}_k^2 = e^{j2\varphi_k}\Big(A_k^2 \beta_k + A_k \mu_k \beta_k - \alpha_k^2 A_k^2 - \alpha_k^2 A_k \mu_k + A_k \mu_k \beta_k + \eta_k \beta_k - \alpha_k^2 A_k \mu_k - \alpha_k^2 \mu_k^2 - \alpha_k^2 A_k^2 - \alpha_k^2 A_k \mu_k + \alpha_k^2 A_k^2 + \alpha_k^2 A_k \mu_k - \alpha_k^2 A_k \mu_k - \alpha_k^2 \mu_k^2 + \alpha_k^2 A_k \mu_k + \alpha_k^2 \mu_k^2\Big) \tag{42}$$

$$= e^{j2\varphi_k}\left(A_k^2 \beta_k + \eta_k \beta_k + 2A_k \mu_k \beta_k - \alpha_k^2 A_k^2 - 2\alpha_k^2 A_k \mu_k - \alpha_k^2 \mu_k^2\right). \tag{43}$$

REFERENCES

[1] O. Lang and M. Huemer, "Classical Widely Linear Estimation of Real Valued Parameter Vectors in Complex Valued Environments," In *arXiv:1704.08825 [math.ST]*, 2017.

[2] D. Lerro and Y. Bar-Shalom, "Tracking with debiased consistent converted measurements versus EKF," In *IEEE Transactions on Aerospace and Electronic Systems*, Vol. 29, No. 3, pp. 1015–1022, Jul 1993.

[3] M. Longbin, S. Xiaoquan, Z. Yiyu, S. Z. Kang, and Y. Bar-Shalom, "Unbiased converted measurements for tracking," In *IEEE Transactions on Aerospace and Electronic Systems*, Vol. 34, No. 3, pp. 1023–1027, Jul 1998.

[4] S. J. Julier and J. K. Uhlmann, "New extension of the Kalman filter to nonlinear systems," In *Proc. SPIE*, Vol. 3068, pp. 182–193, 1997.

[5] ——, "Consistent debiased method for converting between polar and Cartesian coordinate systems," In *Proc. SPIE*, Vol. 3086, pp. 110–121, 1997.

[6] R. Zhan and J. Wan, "Iterated Unscented Kalman Filter for Passive Target Tracking," In *IEEE Transactions on Aerospace and Electronic Systems*, Vol. 43, No. 3, pp. 1155–1163, July 2007.

[7] S. M. Kay, *Fundamentals of Statistical Signal Processing: Estimation Theory*, Vol. 1. Prentice Hall, 1993.

[8] T. Adali, P. Schreier, and L. Scharf, "Complex-Valued Signal Processing: The Proper Way to Deal With Impropriety," In *IEEE Transactions on Signal Processing*, Vol. 59, No. 11, pp. 5101–5125, Nov 2011.

[9] P. Schreier and L. Scharf, *Statistical Signal Processing of Complex-Valued Data: The Theory of Improper and Noncircular Signals*. Cambridge University Press, 2010.

[10] M. F. Bugallo, V. Elvira, L. Martino, D. Luengo, J. Miguez, and P. M. Djuric, "Adaptive importance sampling: the past, the present, and the future," In *IEEE Signal Processing Magazine*, Vol. 34, No. 4, pp. 60–79, 2017.

[11] V. Elvira, L. Martino, D. Luengo, and M. F. Bugallo, "Improving population Monte Carlo: Alternative weighting and resampling schemes," In *Signal Processing*, Vol. 131, pp. 77–91, 2017.

[12] L. Martino, V. Elvira, D. Luengo, and J. Corander, "An adaptive population importance sampler: Learning from uncertainty," In *IEEE Transactions on Signal Processing*, Vol. 63, No. 16, pp. 4422–4437, 2015.

[13] ——, "Layered adaptive importance sampling," In *Statistics and Computing*, Vol. 27, No. 3, pp. 599–623, 2017.